Journal of Materials Chemistry A

Accepted Manuscript

This article can be cited before page numbers have been issued, to do this please use: Y. Liu, Y. Jiang, F. Li, F. Yu, W. Jiang and L. Xia, *J. Mater. Chem. A*, 2018, DOI: 10.1039/C8TA01304G.

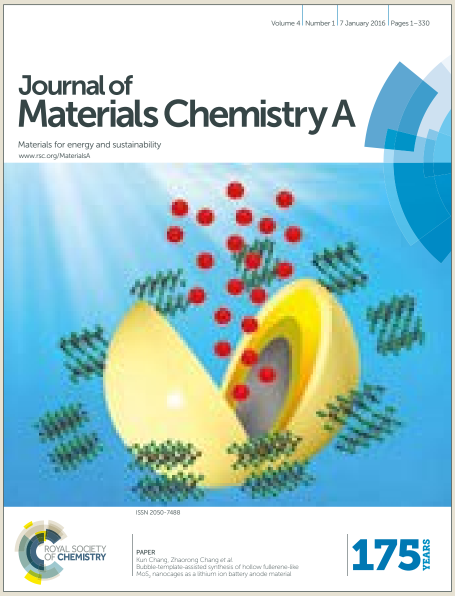

View Article Online
DOI: 10.1039/C8TA01304G

Journal Name

ARTICLE

Molecular Cobalt Salophen Catalyst-Integrated $BiVO_4$ as Stable and Robust Photoanodes for Photoelectrochemical Water Splitting

Received 00th January 20xx,
Accepted 00th January 20xx

DOI: 10.1039/x0xx00000x

www.rsc.org/

Yidan Liu, [a] Yi Jiang,*[a] Fei Li, [b] Fengshou Yu, [b] Wenchao Jiang [a] and Lixin Xia*[a]

Photoelectrochemical (PEC) water splitting is a promising method for the conversion and storage of solar energy. A combination of catalysts with photoelectrodes is generally required in the development of active photoanodes in PEC devices. In this work, we present two $BiVO_4$ photoanodes modified with cobalt salophen (Co(salophen)) complexes for PEC water oxidation. The resulting photoanodes show significantly enhanced PEC performance. Under simulated sunlight illumination (AM 1.5G, 100 mW/cm^2), high photocurrents of 3.89 mA/cm^2 and 4.27 mA/cm^2 were obtained for Co1/$BiVO_4$ and Co2/$BiVO_4$ respectively at 1.23 V (vs. reversible hydrogen electrode (RHE)) in a neutral solution, an almost three-fold enhancement over that of the unmodified $BiVO_4$. Intensity-modulated photocurrent spectroscopy (IMPS) analysises show that the Co(salophen) complexes, not only accelerate the water oxidation reaction, but also reduce the surface recombination. The half-cell solar energy conversion efficiencies for Co1/$BiVO_4$ and Co2/$BiVO_4$ were 1.09% and 1.18% at 0.7 V, respectively. Due to their hydrophobic nature, the Co(salophen) complexes can bind strongly to the surface of $BiVO_4$. When the Co2 complex featuring four hydrophobic tert-butyl groups in salophen ligand was anchored to $BiVO_4$, an extremely stable photocurrent of more than 3.5 mA/cm^2 at 1.23 V vs. RHE is sustained for at least 3 h without decay. Such a stable and robust photoanode based on molecular WOC surpass those attained by most of the state-of-the-art heterogeneous catalysts.

Introduction

Photoelectrochemical (PEC) water splitting to generate hydrogen using sunlight offers an attractive route to achieve the conversion and storage of solar energy.[1-3] In a PEC device, the oxygen evolution reaction (OER) in the photoanode as the key half reaction is generally considered as the bottleneck, due to its multiple electron and proton processes which are thermodynamically demanding.[4-6] Therefore, one of the barriers needed to be overcome prior to a widespread use of this technology is development of stable and efficient photoanodes.[7,8] $BiVO_4$ has been considered a promising candidate due to its appropriate bandgap of 2.4 eV to harvest visible light, and has other merits including abundance, low cost, nontoxicity, and suitable valence band energy for water oxidation.[9,10] However, the PEC performance of unmodified $BiVO_4$ has been limited by its poor charge transport and sluggish water oxidation kinetics. An efficient way to overcome this problem is integrating $BiVO_4$ electrodes with a water oxidation catalyst (WOC).[11-17]

Previous studies have revealed that the immobilisation of inorganic WOCs such as Co-Pi[11,12] and FeOOH/NiOOH[13] can improve the PEC performance of $BiVO_4$. However, these heterogeneous WOCs on the electrode surface have been generally prepared through electrodeposition or photodeposition, and in this process the thickness of the catalyst film must be controlled carefully because of its significant influence on light absorption and charge transport.[18,19] Apart from heterogeneous WOCs, molecular WOCs have recently attracted attention due to their high activity, structural tuneability, and facility in mechanistic studies.[20-23]

However, there are relatively few reports on the combination of $BiVO_4$ photoanodes with a molecular co-catalyst.[24-26] One such recent study by Li and co-workers researched a hybrid photoanode by combining $BiVO_4$ film with a molecular co-cubane catalyst, which gives a high PEC performance.[26] Though in their work, an alkaline condition (pH 9) was required, which is not considered environmentally friendly. Therefore, a molecular catalyst-based photoanode with high activity and stability remains a prerequisite for efficient PEC water splitting under mild and environmentally

---

[a] *College of Chemistry, Liaoning University, Shenyang 110036, Liaoning, China*
**E-mail: jiangyi@lnu.edu.cn; lixinxia@lnu.edu.cn.*
[b] *State Key Laboratory of Fine Chemicals, Dalian University of Technology, Dalian, 116024, China*

Electronic Supplementary Information (ESI) available: [details of any supplementary information available should be included here]. See DOI: 10.1039/x0xx00000x

View Article Online
DOI: 10.1039/C8TA01304G

friendly conditions. Given this, our research reports on two hybrid photoanodes, fabricated by combining molecular Co(salophen) complexes onto a porous $BiVO_4$ surface. Cobalt(II) salophen complexes are easily synthesised and have been well studied in many catalytic fields.[27,28] Recently, a Co(salophen) complex was shown to be an effective water oxidation catalyst either in a homogeneous system or on the electrode surface.[29-32]

In this work, two Co(salophen) complexes (Scheme 1) were directly and physically absorbed onto porous $BiVO_4$ electrodes via hydrophobic interaction. Compared with the conventional loading methods of molecular catalysts, this facile method avoids the high cost by using Nafion[33-35] as the adhesive and the complicated synthetic process required in the introduction of a $-PO_3H_2$ or -COOH binding group.[36-39] The hydrophobic property of the Co(salophen) complex provides a strong binding interaction to the electrode surface rather than dissolving into the solution. The as prepared hybrid photoanodes exhibit excellent PEC activity and stability at neutral pH, which is even higher than those attained by most of the state-of-the-art heterogeneous catalysts. To the best of our knowledge, such a stable and robust hybrid photoanode, based on molecular catalyst in neutral condition, is yet to be reported.

Results and discussion

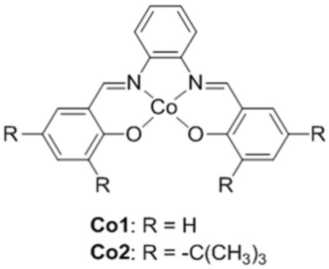

Scheme 1. Structures of the Co(salophen) complexes.

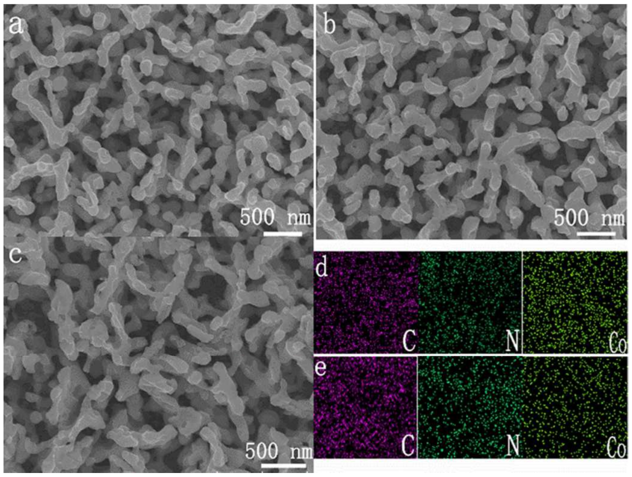

Figure 1. SEM images of (a) $BiVO_4$ electrode, (b) Co1/$BiVO_4$ electrode and (c) Co2/$BiVO_4$ electrode; the elemental mapping of carbon, nitrogen and cobalt by EDX spectroscopy of (d) Co1/$BiVO_4$ electrode and (e) Co2/$BiVO_4$ electrode.

Characterisation of Photoanodes

The $BiVO_4$ thin films on the FTO-coated glass substrates were fabricated by a two-step procedure described previously by Choi and co-workers (see the experimental section for details) and the X-ray diffraction peaks are essentially consistent with that reported previously (Figure S1).[13] The assembled Co(salophen)/$BiVO_4$ electrodes were facilely prepared by soaking the $BiVO_4$ electrode in a solution of Co(salophen) complex in acetonitrile at room temperature, the as-prepared electrodes are referred to as Co1/$BiVO_4$ and Co2/$BiVO_4$. Due to their hydrophobic nature, the Co(salophen) complexes are sufficiently stable when assembled on the surface of $BiVO_4$. Static contact angle measurements (Figure S2) demonstrate that the hydrophobic nature of the electrodes are enhanced after the modification of Co(salophen) complexes (37.1° for Co1/$BiVO_4$, 47.3° for Co2/$BiVO_4$).

Scanning electron microscopy (SEM) was used to observe the morphology of the as prepared electrodes. The bare $BiVO_4$ film shows the appearance of a three-dimensional (3D) network, composed of multiple worm-like nanoparticles (Figure 1a). This nanoporous structure guarantees the adsorption of the molecular catalyst. After the modification with Co(salophen) complexes, the electrodes are retained, and no aggregation or new features are observed (Figures 1b and c). The elemental mapping images indicate that Co is uniformly dispersed on the surface of $BiVO_4$ (Figures 1d and e). The Co 2p spectra in X-ray photoelectron spectroscopy (XPS) show two characteristic peaks at 781 eV and 796 eV, which is belong to the Co 2p3/2 and Co 2p1/2 spin-orbital of Co (II) in Co1 and Co2 (Figures S3). Raman spectroscopy also confirms that Cobalt complexes have been successfully modified on the surface of $BiVO_4$ as the characteristic signal of Cobalt complexes are observed completely (Figure 2). According to the results of inductively coupled plasma spectrometry (ICP), the amount of Co bound to Co1/$BiVO_4$ and Co2/$BiVO_4$ were calculated to be 44.9 $nmol/cm^2$ and 39.7 $nmol/cm^2$, respectively. The difference in the catalyst loading amount is due mainly to steric hindrance, for which Co2 has a larger molecular volume than Co1. With this extent of loading, Co(salophen) complexes have no impact on the light absorption of the original electrode, as is shown in the UV-Vis spectra (Figure S4). This indicates that the molecular catalyst cannot block or reflect the relevant photons in the visible range, which is one of the greatest advantages of using a molecular catalyst over inorganic one.

View Article Online
DOI: 10.1039/C8TA01304G

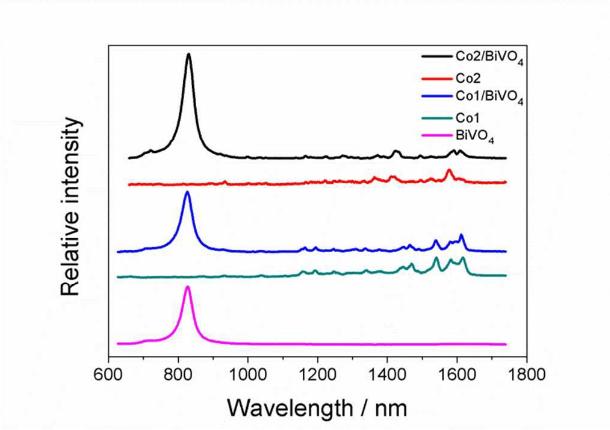

Figure 2. Raman spectra of BiVO$_4$ electrode, Co(salophen) powders, and Co(salophen)/BiVO$_4$ photoelectrodes.

PEC Performance

The PEC performance of the resulting photoanodes was measured in a 0.1 M phosphate buffer solution (pH 7), using simulated sunlight (AM 1.5, 100 mW/cm^2), in a standard three-electrode system with the sample photoanodes as the working electrodes, a platinum wire as the counter electrode, and Ag/AgCl as the reference electrode. First, the electrocatalytic activities for water oxidation of the Co(salophen) complexes on the bare FTO substrate were investigated. The photocurrent-potential (J-V) curves determined by linear sweep voltammetry (LSV) are shown in Figure 3a. Both the two complexes show catalytic activity for water oxidation with a similar onset potential of 1.85 V versus the reversible hydrogen electrode (RHE, all further potentials are reported against RHE unless otherwise stated), which implies an overpotential of 620 mV for Co1 and Co2, respectively. Co2 exhibits higher electrocatalytic activity than Co1, but neither of them is high efficient in electrocatalytic water oxidation, compared to other WOCs. However, under simulated sunlight illumination, the Co(salophen)-modified samples exhibit considerably enhanced photocurrents (Figure 3b). High photocurrents of 3.89 mA/cm^2 and 4.27 mA/cm^2 are obtained for Co1/BiVO$_4$ and Co2/BiVO$_4$ respectively, at an applied potential of 1.23 V. While for the bare BiVO$_4$, the photocurrent at the same potential is only 1.48 mA/cm^2. Moreover, compared to the bare BiVO$_4$, the onset potential is cathodically shifted by more than 200 mV, and the potential at a photocurrent density of 1 mA/cm^2 is cathodically shifted by 600 mV for Co(salophen)-modified BiVO$_4$. The remarkable reduction in onset potential and increase in photocurrent demonstrates that Co(salophen) complexes act as efficient cocatalysts on the surface of the photoanodes in PEC water splitting.

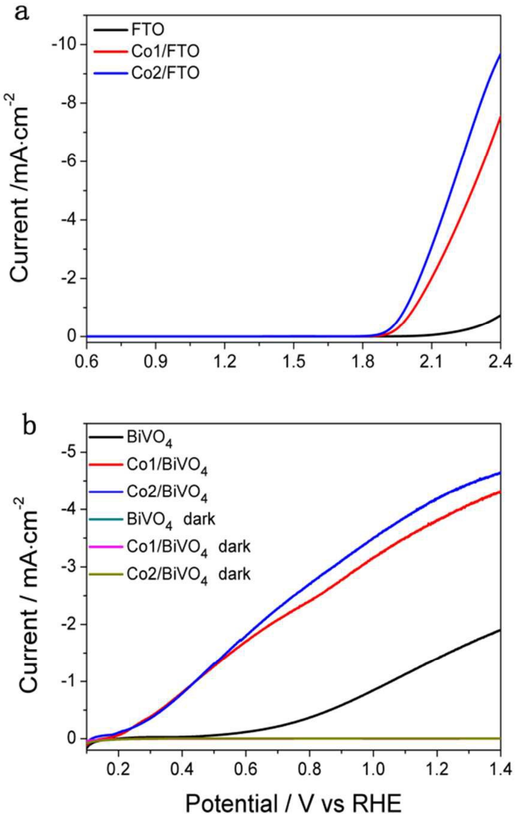

Figure 3. (a) J-V curves of Co1/FTO, Co2/FTO in comparison with the bare FTO under dark condition; (b) J-V curves of Co1/BiVO$_4$ and Co2/BiVO$_4$ in comparison with the bare BiVO$_4$ under AM 1.5G simulated sunlight irradiation.

Based on the LSV results in Figure 3b, the applied bias photon-to-current efficiency (ABPE) for Co1/BiVO$_4$ was calculated, with a maximum value of 1.09% at 0.7 V. The maximum ABPE for Co2/BiVO$_4$ was calculated to be 1.18% at 0.7 V, about eight-fold enhancement over that of unmodified BiVO$_4$ (Figure S5). Figure S6 shows the incident photon-to-current conversion efficiencies (IPCE) on bare and Co(salophen)-modified BiVO$_4$ photoanodes at different wavelengths measured under a bias potential of 1.23 V. With the increasing wavelength, the IPCE value of each sample remains steady before 460 nm after which it decreases, which is consistent with their light absorption. Co(salophen)-modified BiVO$_4$ photoanodes show higher IPCE values than the bare BiVO$_4$. At 430 nm, the IPCE values are around 86% and 89%, for Co1/BiVO$_4$ and Co2/BiVO$_4$, respectively.

To explore the interface charge transport behaviour of the as-prepared photoelectrodes, the photocurrents were measured in the presence of sodium sulfite (Na$_2$SO$_3$) to eliminate the holes injection barrier (Figure S7). The photocurrent density arising from PEC water oxidation can be described as:

$J_{H2O} = J_{abs} \times \eta_{sep} \times \eta_{inj}$,

View Article Online
DOI: 10.1039/C8TA01304G

where: J_{abs} is the photocurrent density when the absorbed photons completely convert into the current, η_{sep} is the charge separation efficiency of the photogenerated holes that refer to the bulk recombination, and η_{inj} is the charge injection efficiency of the surface reaching holes into the electrolyte.[11,13] With Na_2SO_3 as a hole scavenger, the surface recombination is eliminated, so η_{inj} = 1, and the photocurrent density can be described as:

$J_{Na2SO3} = J_{abs} \times \eta_{sep}$.

The bare $BiVO_4$ generates a significantly enhanced photocurrent in the presence of Na_2SO_3 because of the negligible surface recombination. Co1/$BiVO_4$ and Co2/$BiVO_4$ show similar photocurrents to the bare $BiVO_4$. The relative charge separation efficiencies of Co1/$BiVO_4$ and Co2/$BiVO_4$ to $BiVO_4$ are shown in Figure S8, which obtained by dividing J_{Na2SO3} of Co1/$BiVO_4$ and Co2/$BiVO_4$ by J_{Na2SO3} of $BiVO_4$. The approximate separation efficiencies for each photoanode indicate that the modification of Co (salophen) cannot alter the bulk recombination. The η_{inj} for each photoelectrode can be calculated by J_{Na2SO3}/J_{H2O}. It can be seen from Figure 4 that Co(salophen)-modified $BiVO_4$ exhibit higher η_{inj} than the bare $BiVO_4$ over the whole potential range. The η_{inj} at 1.23 V for Co1/$BiVO_4$ and Co2/$BiVO_4$ can reach 89.3% and 92.4%, respectively, whereas that obtained by the bare $BiVO_4$ is only 58.0%. These results confirm that Co(salophen) complexes can effectively restrain the surface recombination and promote hole injection into the electrolyte. But it is not known from this experiment whether the η_{inj} improvement stems from an absolute increase in surface charge transfer (Co(salophen) complex works as an OER catalyst), an absolute decrease in surface recombination (Co(salophen) complex works as a surface passivation cocatalyst), or both.

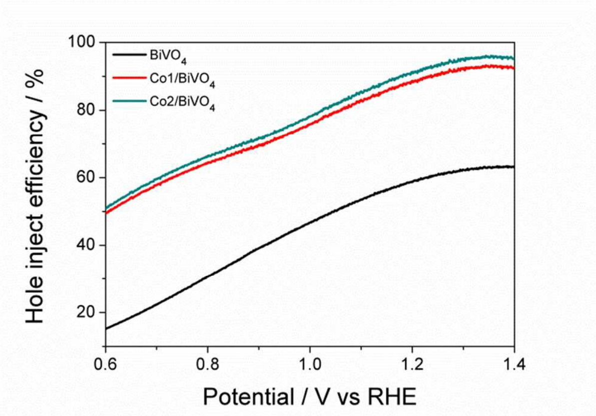

Figure 4. Hole injection efficiencies of Co1/$BiVO_4$ and Co2/$BiVO_4$ in comparison with the bare $BiVO_4$.

Surface Kinetics by IMPS

To understand the real role of Co(salophen) complexes on the photoanodes, intensity modulated photocurrent spectroscopy (IMPS) measurements were employed. This technique has been previously applied to study the charge transfer and surface recombination kinetics of photoanodes.[40-44] Several recent reports on $BiVO_4$ have shown that when Co-Pi was deposited on the $BiVO_4$, it passivates recombination centers rather than works as water oxidation catalyst.[44-46] Figure 5a shows typical IMPS responses of Co1/$BiVO_4$, Co2/$BiVO_4$ and bare $BiVO_4$ in the complex plane. It can be shown that the IMPS response is expressed as a function of frequency. The frequency at the maximum imaginary part corresponds to the sum of the charge transfer (k_{trans}) and recombination (k_{rec}) rate constants ($k_{trans} + k_{rec} = 2\pi f_{max}$). The low frequency intercept in normalized form, at which the imaginary part equals 0 ($Im(j_{photo}/j_h) = 0$), corresponds to the charge transfer efficiency ($k_{trans}/(k_{trans} + k_{rec})$). Thus, the key parameters k_{rec} and k_{trans} at different applied bias potentials are readily obtained.[40] The electron transfer time (τ_d) can be estimated from frequency at the minimum imaginary part ($\tau_d = 1/2\pi f_{min}$).[47]

As shown in Figure 5b, both Co1/$BiVO_4$ and Co2/$BiVO_4$ exhibit higher values of k_{tran} compared to the bare $BiVO_4$ over the entire potential range, indicating that both Co(salophen) complexes perform as OER catalysts on the surface of the photoanodes. The k_{rec} values for each photoanode are shown in Figure 5c. Lower values of k_{rec} are observed for both Co1/$BiVO_4$ and Co2/$BiVO_4$. Additionally, Co2/$BiVO_4$ exhibits a slightly increase in k_{trans} and decrease in k_{rec} than Co1/$BiVO_4$, which is in accordance with its high photocurrent. These results demonstrate that Co(salophen) complexes not only accelerate the water oxidation reaction as OER catalysts, but also reduce the surface recombination, which is in contrast to the mere passivation action of Co-Pi as reported.

The charge transfer efficiencies, defined as $k_{trans}/(k_{trans} + k_{rec})$, are obtained (Figure S9). The enhanced values for Co1/$BiVO_4$ and Co2/$BiVO_4$ are consistent with the η_{inj} as mentioned above. The transfer times of the photoanodes are shown in Figure 5d. Each sample exhibits a decreasing τ_d with the increase of the bias potential. The electron lifetimes of Co1/$BiVO_4$ and Co2/$BiVO_4$ are much shorter (less than half) than that of the bare $BiVO_4$, again supporting their superior charge transfer abilities.

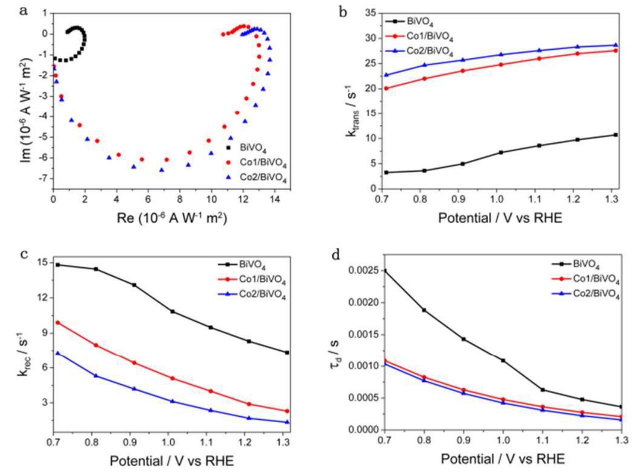

Figure 5. (a) Intensity-modulated photocurrent spectroscopy responses of bare $BiVO_4$, Co1/$BiVO_4$ and Co2/$BiVO_4$ at 1.11 V; (b) Charge transfer rate constants (k_{trans}), (c) Charge recombination rate constants (k_{rec}), (d) Charge transfer times of different photoanodes extracted from IMPS analysis.

View Article Online
DOI: 10.1039/C8TA01304G

Stability

The PEC stability of the photoelectrode is of great importance for a PEC device, especially for a molecular assembled device. In order to check the stability of the photoanodes during PEC water oxidation, a long-term photolysis at 1.23 V under visible-light irradiation was conducted (Figure 6). The unmodified $BiVO_4$ shows a low initial photocurrent density of no more than 1.48 mA/cm^2 and then a rapid decline in photocurrent to less than 0.86 mA/cm^2 within three hours. The decline in photocurrent caused by photocorrosion can be restrained by Co(salophen) complexes. Co1/$BiVO_4$ shows a strong photocurrent followed by a slightly decay. For Co2/$BiVO_4$, a stable photocurrent of more than 3.5 mA/cm^2 is sustained for at least 3 h without decay. Such stable PEC performance is very rare for molecular catalyst-based photoanodes, even surpassing that in most heterogeneous catalyst-based photoanodes.

The high PEC stability of Co1/$BiVO_4$ and Co2/$BiVO_4$ is mainly attributed to the hydrophobic nature of the Co(salophen) complexes. To prove this point, PEC experiments were carried out after soaking the Co(salophen)-modified photoanodes in different solutions overnight. As shown in Figure S10, after soaking treatment in water, the J-V curve is almost unchanged compared with the untreated one. After soaking treatment in ethanol, the J-V curve exhibits a slightly decrease. While after soaking treatment in dichloromethane, the J-V curve decreases significantly, indicating a serious detachment of Co(salophen) complex. Therefore, the hydrophobic nature of the Co(salophen) complexes enables them to maintain on the electrode rather than dissolving into water, which gives rise to a high PEC stability. Co2/$BiVO_4$ exhibits a more stable photocurrent compared with Co1/$BiVO_4$. The tert-butyl group in Co2 improves its hydrophobicity, so that it is more difficult to desorb from the electrode. This is evidenced by ICP measurements. After three hours of photoelectrolysis, the amount of Co on Co1/$BiVO_4$ decreased by 43.4% (from 44.9 $nmol/cm^2$ to 25.4 $nmol/cm^2$), while that on Co2/BiVO4 decreased only by 8.3% (from 39.7 $nmol/cm^2$ to 36.4 $nmol/cm^2$). These results are indicative of a perfect combination of the catalysts and $BiVO_4$.

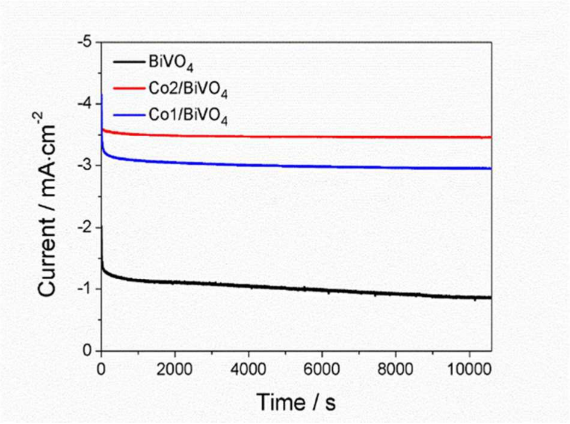

Figure 6. I-t curves of $BiVO_4$ (black), Co1/$BiVO_4$ (blue) and Co2/$BiVO_4$ (red) at 1.23 V vs. RHE.

In order to accurately assess the effect of the molecular Co(salophen) catalysts on actual oxygen production, the evolved O_2 in headspace was quantified by gas chromatography. With a four hour photoelectrolysis, oxygen formed at rates of 6.25 μmol/h, 24.77 μmol/h and 27.78 μmol/h on $BiVO_4$, Co1/$BiVO_4$ and Co2/$BiVO_4$, respectively. Additionally, the stoichiometric ratio of evolved oxygen to hydrogen detected on the counter electrodes was close to 1:2. The faradaic efficiencies of the electrodes were obtained by comparing the actual amount of detected O_2 with the theoretical amount of O_2, which was calculated from the generated photocurrent by assuming that all charges were used for $4e^-$ oxidation of water. As shown in Figure S11, Co1/$BiVO_4$ and Co2/$BiVO_4$ exhibit a significant increase in faradaic efficiency (88% and 91%, respectively) relative to the bare $BiVO_4$ (74%), indicating that by introducing Co(salophen) complexes, more surface arriving holes are utilised through a four-electron transfer process. These results demonstrate that the modification of Co(salophen) complexes on $BiVO_4$ photoanodes as high-performance OER catalysts cannot only increase the photocurrent, but also selectively improve the kinetics of the O_2 evolution reaction.

Real catalyst or catalyst precursor

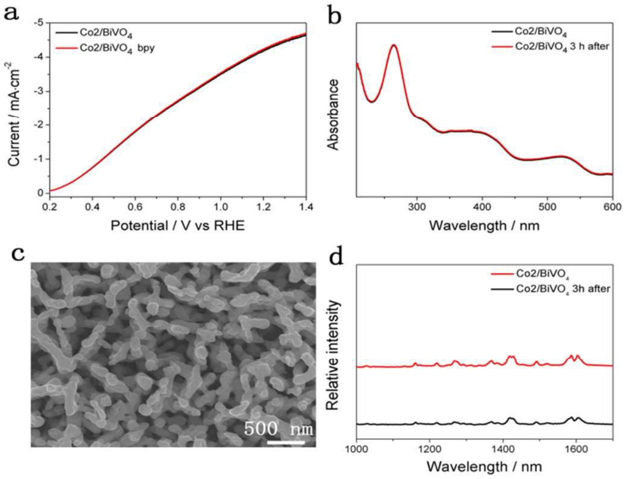

Figure 7. (a) LSV curves of Co2/$BiVO_4$ in 0.1 M phosphate buffer solution with and without bpy (0.1 mM) under AM 1.5G simulated sunlight irradiation; (b) UV-Vis spectra of Co2 in solution before and after 3 h irradiation; (c) SEM images of Co2/$BiVO_4$ after 3 h PEC measurement; (d) Raman spectra of Co2/$BiVO_4$ photoelectrode before and after 3 h PEC measurement.

For molecular WOC, a notable question is whether the complex is a real homogeneous catalyst or only a function as a precursor of the heterogeneous active species.[48-51] To exclude the possibility that the enhancement in PEC performance was due to the Co^{2+} or to formed heterogeneous CoO_x from the dissociation of molecular catalyst, the following experiments were conducted. First, the control experiments were

View Article Online
DOI: 10.1039/C8TA01304G

conducted by using the $BiVO_4$ electrode soaked in a solution containing only cobalt ions or salophen ligand, and no increase in photocurrent density can be observed (Figure S12), suggesting that the Co(salophen) complexes themselves are necessary to improve the PEC performance. Second, a certain amount of 2,2'-bipyridine (bpy) was added into the electrolyte as a chelating agent to clarify the contribution from the probable free cobalt ions released from the Co(salophen) complexes.[26,52,53] As shown in Figures 7a and S13, the presence of bpy has no influence on the photocurrent. Though it cannot completely exclude the existence of the released cobalt ions, it can verify that the improved photocurrent is not owing to free cobalt ions. Moreover, $Co^{2+}/BiVO_4$ exhibits unchanged i-t curve compared with $BiVO_4$ (Figure S14), indicating that even trace amounts of Co^{2+} released from the Co(salophen) complexes, it will not form sufficient CoO_x which can lead to an enhanced photocurrent, which rules out the possibility that the improved photocurrent is due to formed CoO_x nanoparticles by Co^{2+} during the photoelectrolysis. Third, UV-vis measurements for Co(salophen) complexes in solution showed that the complexes were stable from degradation under illumination (Figures 7b and S15). Fourth, if CoO_x or Co-Pi form on the electrode, there is usually an obvious increase or decline in photocurrent.[54-57] However, in this work, the photocurrent is very stable. After a three hour photoelectrolysis, no morphology change and no obvious new nanoparticles are found on the surface of $BiVO_4$ from the SEM images (Figures 7c and S16), indicating that the cobalt complexes did not decompose to form heterogeneous cobalt oxide materials. Fifth, the raman spectra revealed that the signal of the Co(salophen) complexes remain unchanged after photoelectrolysis (Figures 7d and S17), confirming the molecular integrity of the Co(salophen) catalyst on the electrode. Therefore, based on the above results, we speculate that the real catalyst is the molecular Co(salophen) complex itself. On the other hand, this work provides a simple and efficient way to introduce a WOC onto a semiconductor photoanode. Even if the molecular catalyst had partly, or completely changed to other active species, such enhancement and stability of photocurrent are still noteworthy in PEC water oxidation.

Experimental

Chemicals and Reagents

All chemical reagents including $Bi(NO_3)_3 \cdot 5H_2O$, $VO(acac)_2$, p-benzoquinone, o-phenylenediamine, salicylic aldehyde, 3,5-di-tert-butylsalicylaldehyde, and $Co(OAc)_2 \cdot 4H_2O$ were purchased from Aldrich or Aladdin. All other reagents were commercially sourced and used without further purification. The fluorine-doped tin oxide (FTO, surface resistivity of 8-12 Ω sq-1 glass plates were purchased from Zhuhai Kaivo Electronic Components Co., Ltd. Prior to the electrochemical experiments, the FTO plates were cleaned by ultrasonication in deionised water, acetone, and ethanol, respectively, at least three times (5 min).

Synthesis of Co(salophen) complexes

Co(salophen) complexes were synthesised according to a method previously reported.[29,48] First, the salophen ligand was synthesised by adding o-phenylenediamine (5 mmol) and salicyl-aldehyde or 3,5-di-tert-butylsalicylaldehyde (10 mmol) into ethanol (25 mL) at room temperature (RT), and then the mixture of the solutions was refluxed for six hours. The precipitated Schiff-base ligand was filtered, giving the desired product, salophen ligand. The corresponding ligand and $Co(OAc)_2 \cdot 4H_2O$ (molar ratio 1:1.2) were added to ethanol (30 mL). Then the mixture was refluxed for two hours. During refluxing, the colour of the reaction solution changed as opposed to the starting ligand. After cooling to RT, the precipitate was filtered with a Buchner funnel and washed three times each with deionised water and ethanol. The obtained precipitate was dried in a vacuum oven for 10 hours at RT.

Preparation of $BiVO_4$ electrodes

The $BiVO_4$ thin film was prepared by modification of a method reported by Choi and co-workers.[13] Adding $Bi(NO_3)_3 \cdot 5H_2O$ (0.04 M) and KI (0.4 M) to a solution of HNO_3 (50 mL, pH = 1.7). This solution was then mixed with absolute ethanol (20 mL) containing 0.23 M p-benzoquinone, and was vigorously stirred for twenty minutes. A typical three-electrode cell was used for electrodeposition with a FTO working electrode, an Ag/AgCl (3 M KCl) reference electrode, and a platinum counter electrode. Cathodic deposition was performed potentiostatically at -0.1 V vs Ag/AgCl at RT with deposition times of five minutes. The BiOI electrode was then obtained after rinsing with deionised water and air-drying. 0.2 mL of a dimethyl sulfoxide (DMSO) solution containing 0.2 M vanadyl acetylacetonate ($VO(acac)_2$) was placed on the BiOI electrode (1 cm × 1 cm) and heated in a muffle furnace at varying temperatures for two hours in air to convert BiOI to $BiVO_4$. $BiVO_4$ electrodes showing the highest photocurrent were obtained when BiOI electrodes were annealed at 450 ^{o}C (ramping rate = 2 $^{o}C/min$) for two hours. Excess V_2O_5 present in the $BiVO_4$ electrodes was removed by soaking in 1 M NaOH solution for 45 min with gentle stirring. The resulting pure $BiVO_4$ electrodes were rinsed with deionised water and dried at RT.

Fabrication of Co(salophen)/FTO electrode

The Co(salophen) complexes (0.5 mM) were dissolved in acetonitrile with 5% Nafion. After ultrasound for 20 min, 60 μL of the solution was casted onto the FTO, and drying in the air.

Fabrication of Co(salophen)/$BiVO_4$ electrode

View Article Online
DOI: 10.1039/C8TA01304G

The assembled Co(salophen)/$BiVO_4$ electrode was finally obtained by soaking the $BiVO_4$ electrode in an acetonitrile solution containing 0.5 mM Co(salophen) catalyst at RT for 10 hours in the dark, followed by rinsing with excess acetonitrile and drying with N_2. With the same way, we obtained the Co^{2+}/$BiVO_4$ electrode by soaking the $BiVO_4$ electrode in an acetonitrile solution containing 0.5 mM cobalt acetate.

Characterisation

The purity and crystal structure of $BiVO_4$ electrodes were examined by powder X-ray diffraction (Bruker Smart APEX II). Scanning electron microscopy (SEM) images and energy-dispersive X-ray analysis (EDX) spectra of the films were obtained with a SU8000 Schottky field emission scanning electron microscope (SFE-SEM) equipped with a Rontec EDX system. UV-vis absorption spectra were obtained on a Lambda 35 UV-vis spectrophotometer, in which the sample electrode was placed in the centre of an integrating sphere to measure all light reflected and transmitted to accurately assess the absorbance. FTO glass was used as the reference for these absorption measurements. Element content was determined by an inductively coupled plasma mass spectroscopy (ICP, PE-43008300). Raman spectra were collected by raman spectrometer (Renishaw inVia). X-ray photoelectron spectra (XPS) measurements were carried out on the thermo scientific ESCALAB 250 instrument (150 W, spot size of 500 μm and Al Kα radiation at 1486.6 eV) to obtain the surface elements.

Electrochemical and photoelectrochemical methods

Electrochemical experiments were performed in a three-electrode electrochemical cell with a CHI 660E instrument potentialstat (Shanghai Chenhua Instrument Co., Ltd.) at RT. In a three-electrode electrochemical system, the photoanodes were used as working electrodes, with an Ag/AgCl electrode (3 M KCl) as the reference electrode and a platinum wire as the counter electrode. The photoelectrodes were irradiated using a Xe lamp (CEL-HXF300C) equipped with an AM 1.5G-filtered illumination, and the light intensity was calibrated to 100 mW/cm^2. The light irradiation came from the behind the photoelectrodes. J-V curves were obtained by linear sweep voltammetry with a scan rate of 10 mV/s. All measured potentials were converted to RHE ($E_{RHE} = E_{Ag/AgCl}$ + 0.197 V + 0.059 pH). Generally, the electrolyte was a 0.1 M phosphate buffer solution.

IMPS measurements were conducted using a potentiostat (IM6ex, Zahner Company) controlled by a Zahner IMPS electrochemical workstation. Intensity-modulated light was provided by a light-emitting diode (LED) that allowed superimposition of sinusoidal modulation (～10%) on a dc illumination level. The wavelength of light was 426 nm with an average intensity of 10 W m^{-2}.The photocurrent as a function of frequency (from 10 kHz to 100 mHz) was recorded at different potentials. The same three-electrode configuration and electrolyte were employed as given in the PEC characterization section.

The applied bias photon-to-current efficiency (ABPE) was calculated fromthe J-V curve using the equation:

$$ABPE(\%)=\frac{J\times(1.23-V_{bia})}{P_{in}}\times 100\%$$

where: J is the photocurrent density, V_{bias} is the applied bias, and P_{in} is the incident illumination power density (AM 1.5 G, 100 mW/ cm^2).

Incident photon-to-current efficiency (IPCE) at each wavelength was measured at 1.23 V vs. RHE using monochromatic light illumination from a 300 W Xe arc lamp equipped with a CEAULIGHT CEL-IS151 monochromator. The IPCE values have been calculated using the equation:

$$IPCE\ (\%) = \frac{1240\times J}{\lambda\times P_{in}}\times 100\,\%$$

where: J is the photocurrent density (mA/cm^2), λ is the incident light wavelength (nm), and P_{in} is the measured irradiance (mW/cm^2). λ is the incident light wavelength (nm), and P_{in} is the measured irradiance (mW/cm^2).

The evolved oxygen and hydrogen were measured by a Gas Chromatograph 6890A using a thermal conductivity detector and argon as the carrier gas. Prior to the measurement, the electrolyte was degassed by bubbling with high purity Ar for 30 minutes. The faradaic efficiency was calculated by assuming that all of the charges were caused by 4e-oxidation of water to produce O_2.

Conclusions

In summary, two molecular WOC/semiconductor hybrid photoanodes (Co1/$BiVO_4$ and Co2/$BiVO_4$) were prepared by introducing Co(salophen) complexes onto $BiVO_4$ via hydrophobic interaction for PEC water oxidation in neutral water. Co(salophen) complexes gave rise to a remarkable enhancement in the PEC performance by the restraining the surface recombination of the photoanodes. Under AM 1.5G illumination, an impressive transient photocurrent of 4.27 mA /cm^2 was obtained at 1.23 V RHE for Co2/$BiVO_4$, nearly three times higher than the bare $BiVO_4$. Studies on surface kinetics by IMPS measurements demonstrate that Co(salophen) complexes improve the PEC performance by simultaneously accelerating the water oxidation reaction and reducing the surface recombination. Additionally, an extremely stable photocurrent of more than 3.5 mA/cm^2 is sustained for at least three hours without decay. The resulting photoanodes based on molecular WOC achieved robust PEC activity and excellent stability. These results suggest that the rational design of molecular WOC/semiconductor photoanode hold great promise for future applications in efficient solar-fuel conversion.

Conflicts of interest

The authors declare no conflict of interest.

Acknowledgements

DOI: 10.1039/C8TA01304G

This work was supported by the National Natural Science Foundation of China (21401092, 21671089), the Shenyang Natural Science Foundation of China (F16-103-4-00), Scientific Research Fund of Liaoning Province (20170540409).

Notes and references

1 M. Gratzel, *Nature,* 2001, **414**, 338-344.
2 N. S. Lewis, *Science,* 2007, **315**, 798-801.
3 M. G. Walter, E. L. Warren, J. R. McKone, S. W. Boettcher, Q. Mi, E. A. Santori and N. S. Lewis, *Chem. Rev.,* 2010, **110**, 6446-6473.
4 A. Kudo, Y. Miseki, *Chem. Soc. Rev.* 2009, **38**, 253-278.
5 L. Duan, L. Tong, Y. Xu and L. Sun, *Energy Environ. Sci.,* 2011, **4**, 3296-3313.
6 K. J. Young, L. A. Martinl, R. L. Milot, R. C. Snoeberger, V. S. Batlsta, C. A. Schmuttenmaer, R. H. Crabtree and G. W. Brudvig, *Coord. Chem. Rev.,* 2012, **256**, 2503–2520.
7 N. S. Lewis and D. G. Nocera, *Proc. Natl. Acad. Sci. USA,* 2006, **103**, 15729–15735.
8 K. S. Joya, Y. F. Joya, K. Ocakoglu and R. van de Krol, *Angew. Chem. Int. Ed.,* 2013, **52**, 10426–10437.
9 Y. Park, K. J. McDonald and K. S. Choi, *Chem. Soc. Rev.,* 2013, **42**, 2321-2337.
10 A. Kudo, K. Omori and H. Kato, *J. Am. Chem. Soc.,* 1999, **121**, 11459–11467.
11 D. K. Zhong, S. Choi and D. R. Gamelin, *J. Am. Chem. Soc.,* 2011, **133**, 18370–18377.
12 S. K. Pilli, T. E. Furtak, L. D. Brown, T. G. Deutsch, J. A. Turnerc and A. M. Herring, *Energy Environ. Sci.,* 2011, **4**, 5028–5034.
13 T.W. Kim and K.S. Choi, *Science,* 2014, **343**, 990–994.
14 X. Chang, T. Wang, P. Zhang, J. Zhang, A. Li and J. Gong, *J. Am. Chem. Soc.,* 2015, **137**, 8356–8359.
15 J. Gan, X. Lu, B. B. Rajeeva, R. Menz, Y. Tong and Y. Zheng, *ChemElectroChem,* 2015, **2**, 1385-1395.
16 B. Liu, H. -Q. Peng, C. -N. Ho, H. Xue, S. Wu, T. -W. Ng, C. -S. Lee and W. Zhang, *Small,* 2017, **13**, 1701875.
17 E. A. Mohamed, Z. N. Zahran and Y. Naruta, *J. Mater. Chem. A,* 2017, **5**, 6825–6831.
18 F. Yu, F. Li, T. Yao, J. Du, Y. Liang, Y. Wang, H. Han and L. Sun, *ACS Catal.,* 2017, **7**, 1868–1874.
19 G. M. Carroll, D. K. Zhong and D. R. Gamelin, *Energy Environ. Sci.,* 2015, **8**, 577–584.
20 M. D. Karkas, E. V. Johnston, O. Verho and B. Akermark, *Acc. Chem. Res.,* 2014, **47**, 100–111.
21 P. Du and R. Eisenberg, *Energy Environ. Sci.,* 2012, **5**, 6012–6021.
22 L. Duan, A. Fischer, Y. Xu and L. Sun, *J. Am. Chem. Soc.,* 2009, **131**, 10397–10399.
23 J. D. Blakemore, R. H. Crabtree and G. W. Brudvig, *Chem. Rev.,* 2015, **115**, 12974–1300.
24 M. de Respinis, K. S. Joya, H. J. M. De Groot, F. D'Souza, W. A. Smith, R. van de Krol and B. Dam, *J. Phys. Chem. C,* 2015, **119**, 7275–7281.
25 B. Liu, J. Li, H. -L. Wu, W. -Q. Liu, X. Jiang, Z. -J. Li, B. Chen, C. -H. Tung and L. -Z. Wu, *ACS Appl. Mater. Interfaces,* 2016, **8**, 18577–18583.
26 Y. Wang, F. Li, X. Zhou, F. Yu, J. Du, L. Bai and L. Sun. *Angew. Chem. Int. Ed.,* 2017, **56**, 6911–6915.
27 C. W. Anson and S. S. Stahl, *J. Am. Chem. Soc.*, 2017, **139**, 18472–18475.
28 C. W. Anson, S. Ghosh, S. Hammes-Schiffer and S. S. Stahl, *J. Am. Chem. Soc.,* 2016, **138**, 4186–4193.
29 E. Pizzolato, M. Natali, B. Posocco, A. M. Lopez, I. Bazzan, M. D. Valentin, P. Galloni, V. Conte, M. Bonchio, F. Scandola and A. Sartorel, *Chem. Commun.,* 2013, **49**, 9941–9943.
30 M. A. Asraf, H. Younus, C. Ezugwu, A. Mehta and F. Verpoort, *Catal. Sci. Technol.,* 2016, **6**, 4271–4282.
31 Z. Jin, P. Lia and D. Xiao, *J. Mater. Chem. A,* 2016, **4**, 11228–11233.
32 T. Li, J. Qian, Q. Zhou, J. Lin and Y. Zheng, *Dalton Trans.,* 2017, **46**, 13020-13026.
33 R. Brimblecombe, A. Koo, G. C. Dismukes, G. F. Swiegers and L. Spiccia, *J. Am. Chem. Soc.,* 2010, **132**, 2892-2894.
34 L. Li, L. Duan, Y. Xu, M. Gorlov, A. Hagfeldt and L. Sun, *Chem. Commun.,* 2010, **46**, 7307-7309.
35 B. Zhang, F. Li, F. Yu, X. Wang, X. Zhou, H. Li, Y. Jiang and L. Sun, *ACS Catal.,* 2014, **4**, 804-809.
36 G. F. Moore, J. D. Blakemore, R. L. Milot, J. F. Hull, H. Song, L. Cai, C. A. Schmuttenmaer, R. H. Crabtree and G. W. Brudvig, *Energy Environ. Sci.*, 2011, **4**, 2389-2392.
37 C. R. K. Glasson, W. Song, D. L. Ashford, A. Vannucci, Z. Chen, J. J. Concepcion, P. L. Holland and T. J. Meyer, *Inorg. Chem.,* 2012, **51**, 8637–8639.
38 Y. Gao, L. Zhang, X. Ding and L. Sun, Phys. *Chem. Chem. Phys.*, 2014, **16**, 12008-12013.
39 K. L. Materna, R. H. Crabtree and G. W. Brudvig, *Chem. Soc. Rev.*, 2017, **46**, 6099-6110.
40 L. M. Peter, K. G. Wijayantha and A. A. Tahir, *Faraday Discuss.,* 2012, **155**, 309-322.
41 L. Peter, *J. Solid State Electrochem.,* 2013, **17**, 315-326.
42 W. Li, D. He, S. W. Sheehan, Y. He, J. E. Thome, X. Yao, G. W. Brudving, K. Lejaeghere and D. Wang, *Energy Environ. Sci.,* 2016, **9**, 1794–1802.
43 L. Joos, K. Lejiaeghere, J. M. Huck, V. V. Speybroeck and B. Smit, *Energy Environ. Sci.,* 2015, **8**, 2480-2491.
44 C. Zachaus, F. F. Abdi, L. M. Peter and R. V. D. Krol, *Chem. Sci.,* 2017, **8**, 3712–3719.
45 Y. Ma, A. Kafizas, S. R. Pendlebury, F. L. Formal and J. R. Durrant, *Adv. Funct. Mater.*, 2016, **26**, 4951–4906.
46 Y. Ma, F. L. Formal, A. Kafizas, S. R. Pendlebury and J. R. Durrant, *J. Mater. Chem. A,* 2015, **3**, 20649–20657.
47 J. Kruger, R. Plass, M. Gratzel, P. J. Cameron and L. M. Peter, *J. Phys. Chem. B,* 2003, **107**, 7536-7539.
48 J. J. Stracke and R. G. Finke, *ACS Catal.,* 2014, **4**, 909–933.
49 V. Artero and M. Fontecave, *Chem. Soc. Rev.,* 2013, **42**, 2338–2356.
50 S. Fukuzumi and D. Hong, *Eur. J. Inorg. Chem.,* 2014, **2014**, 645–659.
51 X. Wu, F. Li, B. Zhang and L. Sun, *J. Photochem. Photobiol. C: Photochem. Rev.*, 2015, **25**, 71-89.
52 A. Han, H. Jia, H. Ma, S. Ye, H. Wu, H. Lei, Y. Han, R. Cao and P. Du, *Phys. Chem. Chem. Phys.*, 2014, **16**, 11224–11232.
53 J.-W. Wang, P. Sahoo and T.-B. Lu, *ACS Catal.,* 2016, **6**, 5062–5068.
54 M. W. Kanan and D. G. Nocera, *Science*, 2008, **321**, 1072–1075.
55 A. Han, H. Wu, Z. Sun, H. Jia and P. Du, *Phys. Chem. Chem. Phys.*, 2013, **15**, 12534—12538.
56 H. Chen, Z. Sun, X. Liu, A. Han and P. Du, *J. Phys. Chem. C,* 2015, **119**, 8998–9004.
57 B. Huang, Y. Wang, S. Zhan and J. Ye, *Appl. Surf. Sci.,* 2017, **396**, 121-128.

View Article Online
DOI: 10.1039/C8TA01304G

Stable and robust photoanodes were assembled by introduce cobalt salophen complexes onto $BiVO_4$ electrode for PEC water oxidation.